Amino acid–derived surfactants: N. Nakashima, S. Asakuma, T. Kunitake, *J. Am. Chem. Soc*. **107**, 509 (1985); T. Kunitake and N. Yamada, *J. Chem. Soc. Chem. Commun*. **1986**, 655 (1986); T. Kunitake, J.-M. Kim, Y. Ishikawa, *J. Chem. Soc. Perkin Trans.* **2**, 885 (1991); N. A. J. M. Sommerdijk, M. H. L. Lambermon, M. C. Feiters, R. J. M. Nolte, B. Zwanenburg, *Chem. Commun*. **1997**, 455 (1997). Nucleic acid–derived surfactants: H. Yanagawa, Y. Ogawa, H. Furuta, K. Tsuno, *Chem. Lett.* **1988**, 269 (1988); *J. Am. Chem. Soc*. **114**, 3414 (1989). Sugar-derived surfactants: J. H. Fuhrhop and W. Helfrich, *Chem. Rev.* **93**, 1565 (1993), and references therein; R. J. H. Hafkamp, M. C. Feiters, R. J. M. Nolte, *Angew. Chem*. **106**, 1054 (1994).
4. J. C. M. van Hest, D. A. P. Delnoye, M. W. P. L. Baars, M. H. P. van Genderen, E. W. Meijer, *Science* **268**, 1592 (1995).
5. L. Zhang and A. Eisenberg, *ibid.*, p. 1728.
6. L. Zhang, K.Yu, A. Eisenberg, *ibid.* **272**, 1777 (1996).
7. R. J. M. Nolte, *Chem. Soc. Rev.* **23**, 11 (1994).
8. M. Clericuzio, G. Alagona, G. Ghio, P. Salvadori, *J. Am. Chem. Soc*., **119**, 1059 (1997).
9. M. M. Green, R. A. Gross, F. C. Schilling, K. Zero, C. Crosby III, *Macromolecules* **21**, 1839 (1988).
10. For a discussion of other, nonhelical structures, see (*8*) and (*9*).
11. P. C. J. Kamer, R. J. M. Nolte, W. Drenth, *J. Chem. Soc. Chem. Commun.* **1986**, 1789 (1986); *J. Am. Chem. Soc.* **110**, 6818 (1988).
12. The *N*-formyl–protected dipeptides were prepared according to standard protecting and coupling procedures and were converted into the isocyanides by a method developed by I. Ugi and R. Meyr [*Angew. Chem.* **70**, 702 (1958)]. The optical purity could easily be checked by proton NMR spectroscopy, because racemization results in diastereomers with different chemical shifts. Detailed syntheses and physical characterization will be published elsewhere.
13. The homopolymers were prepared by stirring the isocyanides with 4 mole percent of $Ni(ClO_4)_2(H_2O)_6$ in $CHCl_3$ for 6 to 8 hours, after which the polymer was precipitated by adding a tenfold excess of H_2O-MeOH (1/1, v/v).
14. PIAA displayed a negative couplet superimposed on a negative CD band in the region of 250 to 300 nm and a negative optical rotation $[\alpha]^{20}_D = -138°$ [$CHCl_3$, concentration (*c*) 0.1 g/dl]. PIAH showed a very strong positive CD band at about 300 nm and a positive optical rotation $[\alpha]^{20}_D = +541°$ ($CHCl_3$, *c* 0.35). These data indicate a *P* helix for PIAA and an *M* helix for PIAH. The physical and chiroptical properties of PIAH were reported previously [J. M. van der Eijk, R. J. M. Nolte, W. Drenth, A. M. F. Hezemans, *Macromolecules* **13**, 1391 (1980); A. J. M. van Beijnen *et al.*, *ibid.* **16**, 1679 (1983)]. The block copolymers had CD spectra very similar to those of the homopolymers. Optical rotation data: PS_{40}-*b*-$PIAA_{20}$, $[\alpha]^{20}_D = -88°$ ($CHCl_3$, *c* 0.06); PS_{40}-*b*-$PIAH_{20}$, $[\alpha]^{20}_D = +205°$ ($CHCl_3$, *c* 0.05).
15. CHARMm Version 3.0, Revision 92.0911 (Residents and Fellows of Harvard College, Cambridge, MA, 1984, 1992).
16. For a calculation of the structure of poly(isocyanide)s, see C. Kolmarr and R. Hoffman [*J. Am. Chem. Soc.* **112**, 8230 (1990)] and (*8*).
17. The spectroscopic data obtained for **1** perfectly matched the data of Ni(II) carbene complexes previously described (*11*).
18. Amine functionalized poly(styrene) was prepared as reported by J. C. M. van Hest *et al.* [*Chem. Eur. J.* **12**, 1616 (1996)].
19. R. W. Stephany and W. Drenth, *Recl. Trav. Chim. Pays-Bas* **91**, 1453 (1972).
20. The block copolymers were characterized with proton (^{1}H) NMR, ^{13}C NMR, and IR spectroscopy. For example, PS_x-*b*-$PIAA_y$: ^{1}H NMR [in deuterochloroform ($CDCl_3$)]; chemical shift, δ (parts per million relative to internal tetramethylsilane) = 0.73 to 1.22 [*Bu*-(CH_2-CHPh)$_x$; Bu, butyl group; Ph, phenyl group], 1.22 to 1.75 [(CH_2-CHPh)$_x$ + (CN-CH(CH_3)-CONH-CH(CH_3)-CO_2CH_3)$_y$], 1.75 to 2.35 [(CH_2-C*H*Ph)$_x$], 3.42 to 3.90 [(CN-CH(CH_3)-CONH-CH(CH_3)-CO_2CH_3)$_y$], 3.90 to 4.88 [(CN-C*H*(CH_3)-CONH-C*H*(CH_3)-CO_2CH_3)$_y$], 6.28 to 7.25 [(CH_2-CH*Ph*)$_x$]. ^{13}C NMR ($CDCl_3$); δ = 14 [CH_3-CH_2-CH_2-CH_2-(CH_2-CHPh)$_x$], 15 to 19.5 [broad, (CN-CH(CH_3)-CONH-CH(CH_3)-CO_2CH_3)$_y$], 20 to 24.5 [broad, (CN-CH(CH_3)-CONH-CH(CH_3)-CO_2CH_3)$_y$], 22.5 [CH_3-CH_2-CH_2-CH_2-(CH_2-CHPh)$_x$], 27 [CH_3-CH_2-CH_2-CH_2-(CH_2-CHPh)$_x$], 32 [CH_3-CH_2-CH_2-CH_2-(CH_2-CHPh)$_x$], 33.5 to 39.5 (broad, CH_2-O-CH_2-CH_2-CH_2-NH_2), 40 to 46 [broad, (CH_2-CHPh)$_x$], 40.5 [broad, (CH_2-CHPh)$_x$], 46.5 to 48 [broad, (CN-CH(CH_3)-CONH-*C*H(CH_3)-CO_2CH_3)$_y$], 49 to 51 [broad, (CN-CH(CH_3)-CONH-CH(CH_3)-CO_2CH_3)$_y$], 61 to 64 [broad, (CN-*C*H(CH_3)-CONH-CH(CH_3)-CO_2CH_3)$_y$], 68 (broad, CH_2-O-CH_2-CH_2-CH_2-NH_2 + CH_2-O-CH_2-CH_2-CH_2-NH_2), 124 to 127 [broad, (CH_2-CH*Ph*$_{para}$)$_x$], 127 to 129.5 [broad, (CH_2-CH*Ph*$_{ortho+meta}$)$_x$], 145 to 146.5 [broad, (CH_2-CH*Ph*$_{ipso}$)$_x$], 160 to 165 [broad, (CN-CH(CH_3)-CONH-CH(CH_3)-CO_2CH_3)$_y$], 171 to 174 [broad, (CN-CH(CH_3)-CONH-CH(CH_3)-CO_2CH_3)$_y$]. IR (KBr pellet): 698, 1160, 1211, 1535, 1663, 1748, 2928, 3295 cm^{-1}.
21. H. G. J. Visser, R. J. M. Nolte, J. W. Zwikker, W. Drenth, *J. Org. Chem.* **17**, 3139 (1985).
22. TEM was performed on a Philips EM210 microscope at an acceleration voltage of 60 kV. For AFM, a Nanoscope III instrument from Digital Instruments was used, operating in the tapping mode.
23. Samples were deposited from the aqueous dispersions onto copper grids coated with a thin film of polyvinyl formaldehyde plastic. Water was evaporated during a period of 1 to 10 min at atmospheric pressure. The remaining water was drained off, and the grids were shadowed with platinum at an angle of 45°.
24. A similar zigzag pattern has been observed in films of block copolymers of poly(hexyl isocyanate) and poly(styrene) [J. T. Chen, E. L. Thomas, C. K. Ober, G.-P. Mao, *Science* **273**, 343 (1996)].
25. V. N. Malashkevich, R. A. Kammerer, V. P. Efimov, T. Schulthess, J. Engel, *ibid.* **274**, 761 (1996).
26. J. P. Straley, *Phys. Rev. A* **14**, 1835 (1976).
27. M. M. Green *et al.*, *Science* **268**, 1860 (1995).
28. M. Kauranen *et al.*, *ibid.* **270**, 966 (1995).
29. We thank the Department of Macromolecular and Organic Chemistry (E. W. Meijer) of the Technical University Eindhoven for kindly providing some poly(styrene) samples, P. C. J. Kamer for useful suggestions, A. E. Rowan for the molecular modeling studies, M. M. Green for fruitful discussions, J. Gerritsen for the AFM measurements, and H. P. M. Geurts for help with the TEM. Supported by the Netherlands Foundation for Chemical Research with financial aid from the Netherlands Organization for Scientific Research.

5 January 1998; accepted 31 March 1998

Identification of Water Ice on the Centaur 1997 CU26

Robert H. Brown,* Dale P. Cruikshank, Yvonne Pendleton, Glenn J. Veeder

Spectra of the Centaur 1997 CU26 were obtained at the Keck Observatory on 27 October 1997 (universal time). The data show strong absorptions at 1.52 and 2.03 micrometers attributable to water ice on the surface of 1997 CU26. The reflectance spectrum of 1997 CU26 is matched by the spectrum of a mixture of low-temperature, particulate water ice and spectrally featureless but otherwise red-colored material. Water ice dominates the spectrum of 1997 CU26, whereas methane or methane-like hydrocarbons apparently dominate the spectrum of the Kuiper belt object 1993 SC, perhaps indicating different origins, thermal histories, or both for these two objects.

Studies of the physical properties and surface compositions of bodies in the outer solar system can give important clues to the conditions that existed in the early solar system. At the large heliocentric distances of bodies in the outer solar system, materials are expected to be much less modified by heating from the sun than those in the region of the terrestrial planets, thus preserving a less altered record of the chemical and physical properties of the original material from which the solar system formed.

An important suite of bodies in this regard is the small, irregular satellites of the Jovian planets, the Centaurs and the Kuiper belt objects (KBOs), which orbit beyond Neptune. The object designated 1997 CU26 (*1*) is one of the seven known Centaurs. The Centaurs are distinguished dynamically as a group of objects whose orbits cross those of the Jovian planets and whose perihelions lie outside the orbit of Jupiter. As a result, Centaur orbits are dynamically unstable on time scales of about 10^7 years (*2*). Thus, that they are observed at all implies a source of new bodies to replenish those that are lost from the Centaur region by collisions or catastrophic gravitational encounters with the Jovian planets (*2*, *3*). One possible source for these objects is the Kuiper belt (*4*). Therefore, determining the surface composition of objects in both regions is necessary to understand the dynamical and chemical evolution of bodies in the outer solar system.

Reported here are near-infrared spectroscopic observations of 1997 CU26 (*5*), conducted at the W. M. Keck Observatory on

R. H. Brown, Lunar and Planetary Lab and Steward Observatory, University of Arizona, Tucson, AZ 85721, USA. D. P. Cruikshank and Y. Pendleton, NASA Ames Research Center, M.S. N245-6, Moffett Field, CA 94035, USA.
G. J. Veeder, Jet Propulsion Laboratory, California Institute of Technology, Pasadena, CA 91109, USA.
*To whom correspondence should be addressed.

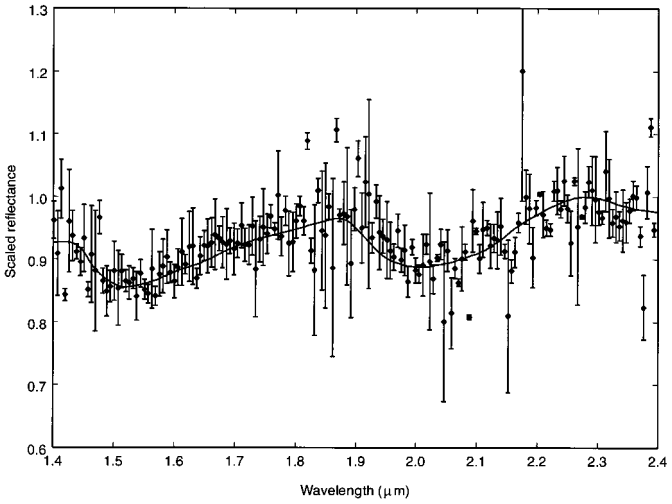

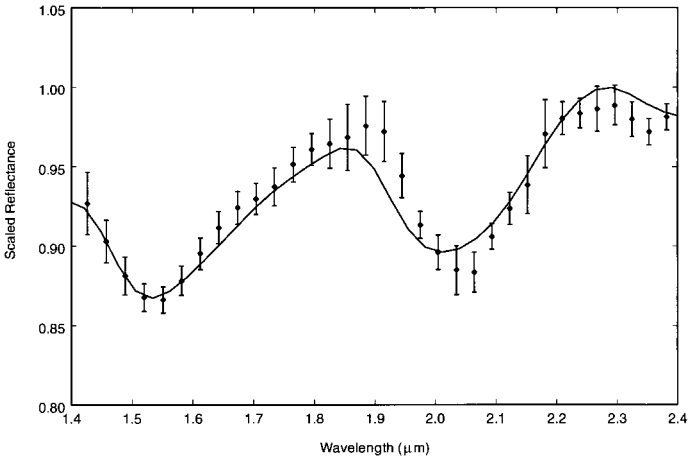

Fig. 1 (Left). The spectrum of 1997 CU26. The error bars are 1σ of the mean. The solid line is a theoretical spectrum of an intimate mixture of particulate water ice and red material (*8–12*) convolved to the same resolution as the data.
Fig. 2 (Right). Low-resolution spectrum of 1997 CU26. The spectrum here was produced by convolving the spectrum in Fig. 1 with a Gaussian whose full width at half maximum is equal to the spacing between 10 channels in the original data (*15, 16*). Also shown is the model from Fig. 1 convolved to the same resolution and with the same sampling interval as the data (solid line).

27 October 1997 (universal time) with the near-infrared camera (NIRC). The spectral measurements were made with the gr120 grism of the NIRC, which has an approximate wavelength range in first order of 1.4 to 2.55 μm and a spectral sampling interval of 0.00607 μm/pixel. The NIRC has an effective pixel size of 0.15 arcsec, and a slit width of 8.5 pixels (~1.3 arcsec) was used for all the spectral observations. Atmospheric seeing was 0.5 arcsec (full width at half maximum) at 2.1 μm, and the air mass range for the observations was 1.32 to 1.42. 1997 CU26 was identified in images with the K_s filter (6), both by its motion and by its predicted position.

Spectra were collected by centering the image of the object in the grism slit and obtaining pairs of images of 1500-s total exposure (20 co-added exposures of 75 s) with each exposure offset along the grism slit by 4 arcsec. Differencing corresponding pairs of images allowed a first-order subtraction of the sky background while providing simultaneous integration on the object and sky. Our spectrum of 1997 CU26 encompasses 3000 s of integration. Correction for telluric extinction and the solar color was accomplished with spectra of the C-type asteroid 156 Xanthippe obtained on the same night and over the same air mass range. Xanthippe has a flat spectrum with no spectral features over the wavelength range of the observations (*7*). The observed spectrum (Fig. 1) and a model spectrum calculated with bidirectional reflectance theory (*8*) and the known optical constants of water ice (*9–11*) both show the strong 1.52- and 2.03-μm absorptions of water ice, which is a conclusive indication of water ice on 1997 CU26.

To reproduce the continuum reflectance of 1997 CU26, we included in the model spectrum a contribution due to a spectrally featureless but otherwise red-colored material, mixed with the water ice. This material has no spectral features (*12*) but was chosen to be an approximate spectral analog for various types of materials (*13*) whose overall reflectance in the 1.4- to 2.4-μm spectral region increases toward longer wavelengths (that is, the material is red colored). Because parameters such as grain sizes of the surface constituents of 1997 CU26 are unknown, the model fit here is neither unique nor quantitative. It is used only for identification of surface constituents.

Within the precision of the full-resolution data, there are no other absorption bands in the spectrum of 1997 CU26 attributable to chemical species other than water ice. Notable also is the weakness of the 1.65-μm absorption that is partially blended with the 1.52-μm absorption in crystalline water ice (*14*). Although no strong conclusion can be drawn from our data, the weakness of this band is consistent with mostly amorphous rather than crystalline water ice on 1997 CU26.

Some chemical species such as methane, ethane, ethylene, and acetylene have absorption bands that are broad enough to be detected at lower spectral resolution than that of our spectrum (given sufficient precision in the data). To check for absorption bands due to other chemical species, we increased the signal-to-noise ratio (SNR) of our spectrum (Fig. 1) at the expense of spectral resolution by convolving it with a Gaussian of 10 spectral channels in width (*15*). This was deemed the best trade-off between increasing the SNR of the spectrum and reducing its spectral resolution. Errors bars were calculated from 1 standard deviation of the mean of each point in the original data propagated through the convolution (*16*).

Convolving the data and the model to lower resolution (Fig. 2) increases the effective SNR, but even with this improvement, the two-component spectral model still fits. There are small deviations between the model and the data, but we attribute them to systematic differences between the optical constants of water ice used for the model calculation and the actual optical constants of the water ice on 1997 CU26. Thus, we conclude that if any other species are present, they do not occur in sufficient quantities, their absorption bands are too narrow, or they are not sufficiently infrared active to show detectable absorption bands in these data.

1997 CU26 and another well-studied Centaur Pholus have water ice on their surfaces (*17*). Pholus has a red color attributed to the presence of organic material and shows evidence of light organic compounds such as methanol (CH_3OH) in its spectrum (*17*). In contrast, our spectrum of 1997 CU26 shows no evidence of light hydrocarbons. The other Centaur for which good spectra have been obtained is 2060 Chiron, whose orbit crosses the orbits of Saturn and Uranus. Chiron has a weak coma and undergoes episodic gas releases like a comet. Its spectrum from 1.4 to 2.4 μm is featureless and nearly flat, similar to that of a C-type asteroid (*18*). Thus, the existing spectral data support the idea that the Centaurs may be compositionally diverse.

The question of the source of supply of the Centaurs is interesting, and some

progress toward an answer may be achieved by comparing the surface composition of the KBO 1993 SC (*19*) with that of 1997 CU26. The spectrum of 1993 SC shows no evidence for water ice unlike that of 1997 CU26 but instead shows evidence for light hydrocarbons such as methane, ethane, ethylene, or acetylene (*19*). This suggests among other possibilities that some of the existing Centaurs have undergone surface modification since they left the Kuiper belt. It also supports the idea that the KBOs may be a compositionally diverse group of objects (*20*, *21*).

Considering only solar system dynamics, it is difficult to escape the conclusion that the Kuiper belt is the source of the Centaurs (*2*, *3*). Thus, the idea that at least some of the Centaurs have undergone substantial surface modification since leaving the Kuiper belt is attractive. One possible mechanism for such surface modification would be preferential sublimation of more volatile species, leaving less volatile species behind as a lag deposit. At the roughly 90 to 95 K present average surface temperature of an object like 1997 CU26 (*11*), one would expect that light hydrocarbons would be preferentially lost whereas water ice and heavier hydrocarbons would be retained. In addition, the closer proximity to the sun of the Centaurs relative to their presumed genesis zone would result in an increased flux of solar ultraviolet radiation on their surfaces with an accompanying increase in the rate of surface photochemical reactions. Those processes would tend to convert light hydrocarbons to heavy hydrocarbons (*13*), increasing any existing surface stock of heavy hydrocarbons. If the Kuiper belt is indeed the source of the short-period comets (*2*, *3*), then the possible presence of heavy hydrocarbons on the Centaurs, like the short-period comets (*20*), would at least be consistent with their originating in the Kuiper belt.

REFERENCES AND NOTES

1. *Minor Planet Circ. 31010* (1997).
2. M. Duncan, T. Quinn, S. Tremaine, *Astrophys. J. Lett.* **328**, L69 (1988); B. Gladman and M. Duncan, *Astron. J.* **100**, 1680 (1990); M. J. Holman and J. Wisdom, *ibid.* **105**, 1987 (1993); M. Irwin, S. Tremaine, A. Zytkow, *ibid.* **110**, 3082 (1995).
3. D. Jewitt, J. Luu, J. Chen, *ibid.* **112**, 1225 (1996).
4. G. P. Kuiper, in *Astrophysics* (McGraw-Hill, New York, 1951), pp. 357–424; K. E. Edgeworth, *Mon. Not. R. Astron. Soc.* **109**, 600 (1948).
5. 1997 CU26 is in a moderately eccentric orbit of inclination 23.4°, lying mostly between Saturn and Uranus. Its aphelion distance is 18.36 astronomical units (AU), barely inside the orbit of Uranus. Its estimated diameter is 440 km, comparable to Uranus' satellite Miranda and Neptune's satellite Nereid. The orbital period of 1997 CU26 is 62.9 years.
6. K_s is the K short filter whose passband encompasses the short-wavelength half of the standard K band.
7. D. J. Tholen, in *Asteroids II* (Univ. of Arizona Press, Tucson, AZ, 1989), pp. 1139–1150; J. F. Bell, B. R. Hawke, P. D. Owensby, M. J. Gaffey, *Lunar Planet. Sci. Conf.* **XIX**, 57 (1988).
8. B. Hapke, in *Remote Geochemical Analyses: Elemental and Mineralogical Composition* (Cambridge Univ. Press, New York, 1993), pp. 31–41.
9. S. Warren, *Appl. Opt.* **23**, 1206 (1984).
10. O. B. Toon, M. A. Tolbert, B. G. Koehler, A. M. Middlebrook, J. Jordan, *J. Geophys Res.* **99**, 25631 (1994).
11. The optical constants of water ice used here were taken from (*9*) and shifted in wavelength to agree with (*10*). The data of (*9*) were deemed to be more precise in the 1.4- to 2.4-μm wavelength region than those in (*10*), but the central wavelengths of the absorption bands in (*10*) corresponded more closely with those of water ice at the 90 to 95 K estimated average present surface temperature of 1997 CU26. This temperature range was calculated assuming a spherical body, a 5 to 20% bolometric bond albedo, instantaneous equilibrium with sunlight, a mean solar zenith angle of $\sqrt{2/\pi}$, and a heliocentric distance of 13.7 AU.
12. The optical constants for the red material were derived by assuming a real index of refraction of 1.4 at a wavelength of 1.0 μm and a Lambert absorption coefficient that increased linearly toward longer wavelengths. These quantities were processed through a subtractive Kramers-Kronig algorithm giving the real indices of refraction corresponding to the defined imaginary indices and the real index in the visual. The calculated reflectance for 10-μm grains gives a roughly linear increase in reflectance from 7.5% at 1.0 μm to 9% at 2.5 μm
13. C. Sagan, B. N. Khare, J. S. Lewis, in *Satellites*, J. A. Burns and M. S. Matthews, Eds. (Univ. of Arizona Press, Tucson, AZ, 1984), pp. 788–807.
14. U. Fink and G. T. Sill, in *Comets*, L. Wilkening, Ed. (Univ. of Arizona Press, Tucson, AZ, 1982), pp. 164–202.
15. The convolution was done as a direct, discrete, numerical-integral convolution (not as a Fourier convolution). The purpose is to model data obtained at intrinsically lower spectral resolution (with the associated increase in SNR due to the larger spectral bandpass). In contrast to the common practice of binning data, which is mathematically equivalent to a discrete convolution with a square wave, the bandpass of most grating and grism spectrometers is very nearly Gaussian; thus, the result is a much better approximation to spectral data obtained at intrinsically lower spectral resolution.
16. The uncertainties were estimated by propagating the error bars of the high-resolution data directly through the convolution (*15*). Photon shot noise from the sky background is expected to be the dominant noise source, but, because the contributions of all the noise sources are not known, a correction for the photon shot noise difference expected in the wider bandpass of the convolved data was not included in the calculation.
17. D. P. Cruikshank *et al.*, in preparation.
18. D. P. Cruikshank, in *From Stardust to Planetesimals*, Y. J. Pendleton and A. G. G. M. Tielens, Eds. (Astronomical Society of the Pacific, San Francisco, CA, 1997).
19. R. H. Brown, D. P. Cruikshank, Y. Pendleton, G. J. Veeder, *Science* **276**, 937 (1997).
20. J. X. Luu, D. C. Jewitt, E. Cloutis, *Icarus* **109**, 133 (1994).
21. J. X. Luu and D. C. Jewitt, *Astrophys. J.* **494**, L117 (1998); D. C. Jewitt and J. X. Luu, in preparation.

22. The W. M. Keck Observatory is operated as a scientific partnership between the California Institute of Technology and the University of California. It was made possible by the generous financial support of the W. M. Keck Foundation. The authors acknowledge the assistance of R. Mastrapa at the telescope and the financial support of NASA through the various grants and contracts that support the authors' work.

15 January 1998; accepted 8 April 1998

Impairment of Mycobacterial Immunity in Human Interleukin-12 Receptor Deficiency

Frédéric Altare, Anne Durandy, David Lammas, Jean-François Emile, Salma Lamhamedi, Françoise Le Deist, Pam Drysdale, Emmanuelle Jouanguy, Rainer Döffinger, Françoise Bernaudin, Olle Jeppsson, Jared A. Gollob, Edgar Meinl, Antony W. Segal, Alain Fischer, Dinakantha Kumararatne, Jean-Laurent Casanova*

In humans, interferon γ (IFN-γ) receptor deficiency leads to a predisposition to mycobacterial infections and impairs the formation of mature granulomas. Interleukin-12 (IL-12) receptor deficiency was found in otherwise healthy individuals with mycobacterial infections. Mature granulomas were seen, surrounded by T cells and centered with epithelioid and multinucleated giant cells, yet reduced IFN-γ concentrations were found to be secreted by activated natural killer and T cells. Thus, IL-12–dependent IFN-γ secretion in humans seems essential in the control of mycobacterial infections, despite the formation of mature granulomas due to IL-12–independent IFN-γ secretion.

Bacille Calmette-Guérin (BCG) and nontuberculous mycobacteria (NTM) are poorly virulent mycobacteria that may cause disseminated disease in otherwise healthy children (*1*–*3*). The identification of inherited IFN-γ receptor ligand-binding chain (IFN-γR1) deficiency provided the first genetic etiology for this syndrome (*4*) and highlighted the importance of IFN-γ, a pleiotropic cytokine secreted by natural killer (NK) and T cells (*5*), in the control of mycobacteria in humans. The lack of mature mycobacterial granulomas showed that their formation is strictly IFN-γ–dependent. Partial, as opposed to complete, IFN-γR1 deficiency is associated with mature granulomas and a milder course of mycobacterial infection (*6*). However, a number